Journal of Alloys and Compounds 572 (2013) 43–48

Contents lists available at SciVerse ScienceDirect

Journal of Alloys and Compounds

journal homepage: www.elsevier.com/locate/jalcom

# Metallurgical and thermoelectric properties in $Co_{1-x}Pd_xSb_3$ and $Co_{1-x}Ni_xSb_3$ revisited

E. Alleno *, E. Zehani [1], O. Rouleau

*ICMPE-CMTR, UMR7182 CNRS – UPEC, 2-8 rue Henri Dunant, 94320 Thiais, France*

ARTICLE INFO

*Article history:*
Received 1 February 2013
Received in revised form 21 March 2013
Accepted 22 March 2013
Available online 29 March 2013

*Keywords:*
Thermoelectricity
Skutterudite
Band gap
Effective mass
Power factor

ABSTRACT

Polycrystalline thermoelectric $Co_{1-x}M_xSb_3$ (M = Ni, Pd) skutterudites have been synthesized by melting, annealing, and spark plasma sintering. The solubility limit of Pd and Ni are determined to be respectively $x_{max} = 0.03$ and $x_{max} = 0.09$. The density of states effective masses range between $2.0m_0$ and $4m_0$ in $Co_{1-x}Pd_xSb_3$ and $Co_{1-x}Ni_xSb_3$. These values are consistent with the effective band mass ($0.3m_0$) and the degeneracy number $N_v = 36$ derived from band structure calculations. Power factor measurements and calculations in $Co_{1-x}Pd_xSb_3$ show that at 300 K, the optimum electron concentration would be $[n]_{opt} = 1.4 \times 10^{20}$ cm$^{-3}$, slightly beyond the electron concentration ($1.1 \times 10^{20}$ cm$^{-3}$) of the solubility limit composition $Co_{0.97}Pd_{0.03}Sb_3$. The maximum power factor is effectively obtained for the composition $Co_{0.97}Pd_{0.03}Sb_3$ and reaches 4.3 mW m$^{-1}$ K$^{-2}$ at 700 K. An activation energy, which can correspond to the intrinsic gap $\varepsilon_G = 0.13$ eV, is determined in $Co_{0.98}Ni_{0.02}Sb_3$. $Co_{1-x}Ni_xSb_3$ displays smaller electronic mobilities than in $Co_{1-x}Pd_xSb_3$ leading to smaller power factors. Best properties (3.4 mW m$^{-1}$ K$^{-2}$) are observed at 700 K in $Co_{0.95}Ni_{0.05}Sb_3$–$Co_{0.94}Ni_{0.06}Sb_3$.



## 1. Introduction

$Co_{1-x}M_xSb_3$ (M = Ni, Pd) skutterudites are *n*-type thermoelectric materials [1–5]. In these solid solutions, Ni and Pd play the role of electron donors and their composition *x* controls the electrons concentration. They crystallize in the cubic $CoAs_3$ structure type (Im-3) with Sb octahedra surrounding the Co/M atoms forming a cubic network. They display thermoelectric power factors as high as $\alpha^2/\rho \sim 3$ mW m$^{-1}$ K$^{-2}$ at 300 K and figure of merit as high as $ZT = \alpha^2 T/\rho\lambda = 0.8$ at 800 K [3] ($\alpha$ the Seebeck coefficient, $\rho$ the resistivity and $\lambda$ the thermal conductivity). Despite these high values of ZT, their thermal conductivity is in the range 6–9 W m$^{-1}$ K$^{-1}$ at 300 K and it is dominated by the phonon contribution. The $Co_{1-x}M_xSb_3$ (M = Ni, Pd) do not display the best figure of merit among *n*-type skutterudites: partially filled skutterudites $A_yCo_4Sb_{12}$ (A = alkaline, alkaline-earth, rare earth) display values of figure of merit at 800 K ranging from ZT = 0.4 in $Nd_{0.1}Co_4Sb_{12}$ [6], ZT = 1.3 in $Yb_{0.25}Co_4Sb_{12}$ [7] and up to ZT = 1.7 in multi-filled $Ba_{0.08}La_{0.05}Yb_{0.04}Co_4Sb_{12}$ [8]. However, because of their apparent simplicity and reduced sensitivity to oxidation, the $Co_{1-x}M_xSb_3$ (M = Ni, Pd) have more often been considered as candidate for nanostructuring (reduced size grain and/or second phase nanoprecipitates) [5,9–12]. In all these cases, the objective of nanostructuring was to reduce the lattice thermal conductivity and not to affect the power factor. This last quantity is determined by the electron concentrations which is controlled by the quantity of dopant (M = Ni, Pd). It is thus important to know in detail the $Co_{1-x}M_xSb_3$ (M = Ni, Pd) systems to chose the composition corresponding to the largest power factor, prior to any nanostructuring operation. If the $Co_{1-x}Ni_xSb_3$ system has been studied by several groups [3–5], the $Co_{1-x}Pd_xSb_3$ system has been studied by only two groups [1–3] who reported a limited set of temperature data [1]. We thus re-examined the metallurgy and electronic transport properties of $Co_{1-x}Pd_xSb_3$ and compared it to $Co_{1-x}Ni_xSb_3$.

## 2. Experiment

The $Co_{1-x}M_xSb_3$ (M = Pd, Ni) polycrystalline samples (3.5 g) were prepared by melting the elements (Co 99.99%, Pd 99.9%, Ni 99.99%, Sb 99.999%) in stoichiometric quantity at 1100 °C during 24 h and annealing at 820 °C during 96 h in vitreous carbon crucibles sealed in a quartz tube. No mass loss larger than 1 mg could be detected. The buttons were finely crushed in an agate mortar and passed through a 36 μm sieve. The powders were then densified by SPS in graphite dies and punches for 10 min at 620 °C under 50 MPa in a SPS Syntex DR SINTER Lab 515S system. Disk- and bar-shaped samples were cut with a diamond saw for transport measurements. The density of the compacts was determined by measuring the geometrical volume of polished disk-shaped samples cut for transport measurements: its relative value was in every case larger than 98%. The samples were individually characterized by X-ray powder diffraction (XRD) using the Rietveld method. The main refined parameters were the Sb (0, *y*, *z*) coordinates and the lattice parameter *a*. A good accuracy, better than $4 \times 10^{-4}$ Å, was achieved by making use of silicon NIST SRM 640 as an internal reference. Secondary phases percentages are X-ray lines

* Corresponding author. Tel.: +33 1 49 78 12 37; fax: +33 1 49 78 12 03.
*E-mail address:* eric.alleno@icmpe.cnrs.fr (E. Alleno).
[1] Present address: GEMaC, Université Versailles-Saint-Quentin, 45, avenue des Etats Unis – Bâtiment Fermat, 78035 Versailles, France.

0925-8388/$ - see front matter © 2013 Elsevier B.V. All rights reserved.
http://dx.doi.org/10.1016/j.jallcom.2013.03.206

intensity ratios: attempts to Rietveld – refine these phases did not improved the accuracy of these percentages, given their small amount. Hot temperature resistivity (van der Pauw, four-probe) and Seebeck coefficient measurements were carried out between 300 K and 800 K with a thermal gradient $\Delta T \sim 2$ K using a homemade apparatus. The estimated relative uncertainties on the measurement of $\alpha$ and $\rho$ are respectively 5% and 5%, giving a relative uncertainty of 11% for the power factor (root of the sum of square of each independent uncertainty). The Hall effect measurements were carried out at 300 K in a PPMS (DC mode) in the van der Pauw geometry by varying the magnetic field between −5T and +5T. The Hall coefficient is then given by the relation $R_H = t \times \Delta U/i\Delta B$ with $t$ the sample thickness, $i$ the current and $\Delta U/\Delta B$ the slope of the Hall voltage versus magnetic field. The electron concentration is then derived from the relation $[n] = -1/e \times R_H$ with e the electron charge, making the assumption that a single parabolic band describes well these systems. The Hall mobility ($\mu$) can be expressed as a function of $R_H$ and $\rho$: $\mu = R_H/\rho$.

## 3. Results and discussion

### 3.1. Lattice parameter and electron concentration

Fig. 1 (top panel) shows the lattice parameters ($a$) of the $Co_{1-x}Pd_xSb_3$ series of samples as a function of the nominal composition $x$. A linearly increases in $Co_{1-x}Pd_xSb_3$ until the value $x = 0.027 \pm 0.006$ is reached. For larger $x$, $a$ still linearly increases with $x$ but with a much smaller slope. Fig. 1 (bottom panel) shows the Hall electron concentration ($[n]$) as a function of $x$ in $Co_{1-x}Pd_xSb_3$. It also linearly increases as a function of $x$ until $x = 0.030 \pm 0.003$ is reached where it linearly decreases. Both these central values and confidence intervals derived from the $a(x)$ and $[n](x)$ data are consistent but because of its smaller uncertainty, we favour the Hall concentration result which indicate that the solubility limit of Pd in $CoSb_3$ is $x_{max} = 0.030$. Tashiro et al. [2] and Anno et al. [3] respectively proposed 0.04 and 0.05 as the solubility limit of Pd in $CoSb_3$. Our work shows that these former values are significantly overestimated. The effect of the solubility limit is also reflected in the content of the secondary phases. For $x \leqslant 0.03$, 1–2% $CoSb_2$ and 0.2% metastable cubic Sb [13] are typical impurity phases found in the corresponding X-ray pattern. For $x \geqslant 0.04$, in addition to the already mentioned secondary phases, increasing quantities of rhombohedral Sb (3% for $x = 0.07$) and cubic $PdSb_2$ (1.5% for $x = 0.07$) could be detected. It is currently difficult to interpret the linear decrease of $[n]$ for $x$ larger than the solubility limit because of the change in the nature of the secondary phases which can contribute to the Hall signal. Rhombohedral Sb is a semi-metal with equal numbers of electrons and holes if pure, but with anisotropic and unequal mobilities of the two types of charge carriers [14]. $PdSb_2$ is reported as a metal with unknown type of dominant charge carriers [15]. Despite their small concentration, the two extra phases can significantly affect the apparent electron concentration since Sb displays large charge carrier mobilities ($0.1–4 \times 10^3$ cm$^2$ V$^{-1}$ s$^{-1}$) and $PdSb_2$ should display a large charge carrier concentration. Nonetheless, indications on the intrinsic electron concentration beyond the solubility limit in $Co_{1-x}Pd_xSb_3$ can be derived from the Seebeck coefficient displayed in Fig. 2. It clearly saturates for $x > 0.03$, which allows excluding significant electron concentration change arising from intrinsic changes in the chemical formula of $Co_{1-x}Pd_xSb_3$ such as interstitials or vacancies in this Pd concentration range. It is thus difficult to provide a well defined reason for the small increase of $a(x)$ for $x > 0.03$ if no drastic chemical changes occur. We can only speculate on micro-structural effect such as micro-stress arising from the secondary phases, which could indeed be at play in this case.

The lattice parameter of $Co_{1-x}Ni_xSb_3$ shown in Fig. 1 (top panel) also linearly increases with the composition $x$ until $x = 0.091 \pm 0.005$ is reached. For larger Ni concentration, the lattice parameter saturates. A break point is also found at $x = 0.092 \pm 0.005$ in the electron concentration versus $x$ curve shown in Fig. 1 (bottom panel). The solubility limit is thus $x_{max} = 0.091 \pm 0.005$. This time, our value is in line with previous values published in the literature: $x_{max} = 0.1$ was reported in Ref. [3] and in Ref. [5]. The nature of the secondary phases also changes at $x_{max}$. For $x \leqslant 0.09$, 0–1% CoSb and 0.2% metastable cubic Sb [13] are typical secondary phases while for $x \geqslant 0.12$, from 1% to 2% rhombohedral Sb and from 1.5% to 5% $NiSb_2$ are additional impurity phases. Contrary to $Co_{1-x}Pd_xSb_3$, $a(x)$ saturates in $Co_{1-x}Ni_xSb_3$

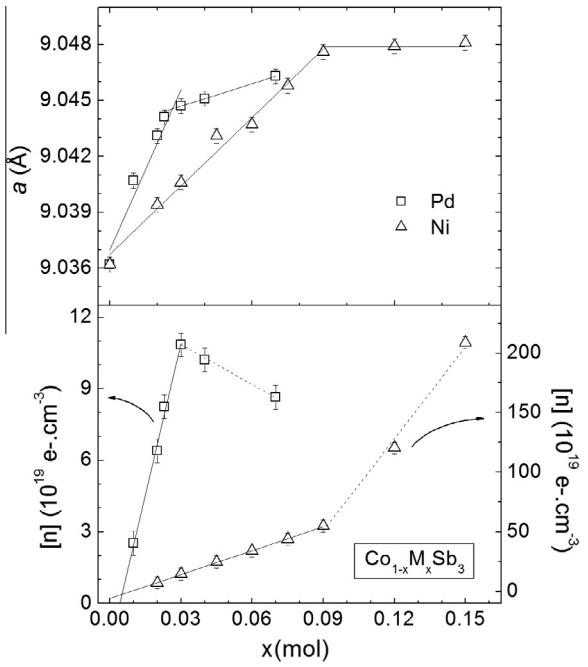


**Fig. 1.** Top panel: lattice parameter of the series $Co_{1-x}Pd_xSb_3$ and $Co_{1-x}Ni_xSb_3$ as a function of the composition $x$. The solid lines are linear regression to the experimental data (see text). Bottom panel: Room temperature Hall electron concentration in $Co_{1-x}Pd_xSb_3$ and $Co_{1-x}Ni_xSb_3$ as a function of the composition $x$. Please note the different vertical scales for $Co_{1-x}Pd_xSb_3$ and $Co_{1-x}Ni_xSb_3$.

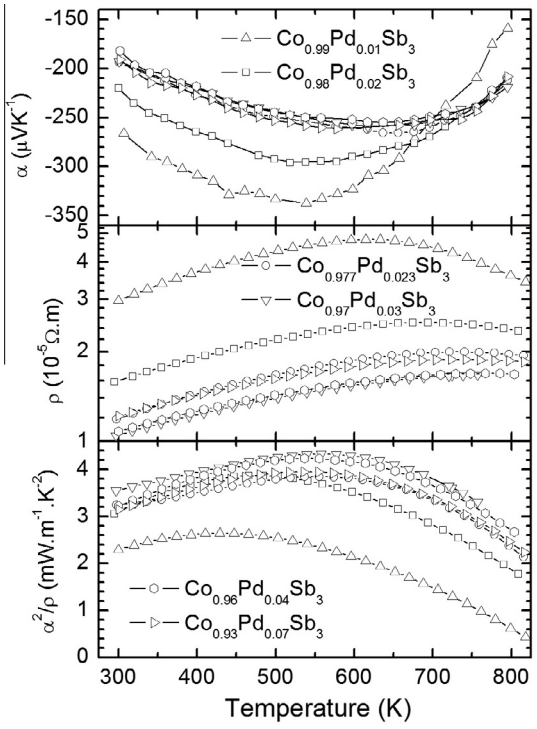


**Fig. 2.** Electronic transport properties as a function of temperature in $Co_{1-x}Pd_xSb_3$. Top panel: Seebeck coefficient; middle panel: electrical resistivity; bottom panel: power factor. Please note the logarithmic scale for the resistivity.